

# Characterization of anti-CD20 monoclonal antibody produced by transgenic silkworms (*Bombyx mori*)

Minoru Tada<sup>1,†,\*</sup>, Ken-ichiro Tatematsu<sup>2,†</sup>, Akiko Ishii-Watabe<sup>1</sup>, Akira Harazono<sup>1</sup>, Daisuke Takakura<sup>1,3</sup>, Noritaka Hashii<sup>1</sup>, Hideki Sezutsu<sup>2</sup>, and Nana Kawasaki<sup>1</sup>

<sup>1</sup>Division of Biological Chemistry and Biologicals; National Institute of Health Sciences; Tokyo, Japan; <sup>2</sup>Transgenic Silkworm Research Unit; National Institute of Agrobiological Sciences; Ibaraki, Japan; <sup>3</sup>Manufacturing Technology Research Association of Biologics; Kobe, Japan

<sup>†</sup>These authors contributed equally to this work.

**Keywords:** monoclonal antibody, transgenic silkworm, ADCC, N-glycosylation, rituximab

**Abbreviations:** mAb, monoclonal antibody; ADCC, antibody-dependent cell-mediated cytotoxicity; CBB, Coomassie Brilliant Blue; CDC, complement-dependent cytotoxicity; CHO, Chinese hamster ovary; MSG, middle silk gland; PBMC, peripheral blood mononuclear cell; SDS-PAGE, sodium dodecyl sulfate-polyacrylamide gel electrophoresis.

In response to the successful use of monoclonal antibodies (mAbs) in the treatment of various diseases, systems for expressing recombinant mAbs using transgenic animals or plants have been widely developed. The silkworm (*Bombyx mori*) is a highly domesticated insect that has recently been used for the production of recombinant proteins. Because of their cost-effective breeding and relatively easy production scale-up, transgenic silkworms show great promise as a novel production system for mAbs. In this study, we established a transgenic silkworm stably expressing a human-mouse chimeric anti-CD20 mAb having the same amino acid sequence as rituximab, and compared its characteristics with rituximab produced by Chinese hamster ovary (CHO) cells (MabThera<sup>®</sup>). The anti-CD20 mAb produced in the transgenic silkworm showed a similar antigen-binding property, but stronger antibody-dependent cell-mediated cytotoxicity (ADCC) and weaker complement-dependent cytotoxicity (CDC) compared to MabThera. Post-translational modification analysis was performed by peptide mapping using liquid chromatography/mass spectrometry. There was a significant difference in the N-glycosylation profile between the CHO- and the silkworm-derived mAbs, but not in other post-translational modifications including oxidation and deamidation. The mass spectra of the N-glycosylated peptide revealed that the observed biological properties were attributable to the characteristic N-glycan structures of the anti-CD20 mAbs produced in the transgenic silkworms, i.e., the lack of the core-fucose and galactose at the non-reducing terminal. These results suggest that the transgenic silkworm may be a promising expression system for the tumor-targeting mAbs with higher ADCC activity.

## Introduction

Recombinant monoclonal antibodies (mAbs) have proven highly successful in various therapeutic applications, including the treatment of cancer, inflammatory diseases and infections.<sup>1–4</sup> For the production of mAbs and other biopharmaceuticals, it is important to select a suitable cell type as substrate. In the case of therapeutic mAbs and other glycoprotein biopharmaceuticals, mammalian cells are commonly used.<sup>5,6</sup> Among the various mammalian cells used as substrates, Chinese hamster ovary (CHO) cells are among the best-characterized, and thus many of

the approved therapeutic mAbs are produced in CHO cells.<sup>5,7</sup> At the same time, in order to lower the cost of production, alternative production systems using transgenic animals<sup>8–10</sup> or transgenic plants<sup>11,12</sup> are also being developed. A recombinant human antithrombin alfa (ATLyn<sup>®</sup>) produced in transgenic goats has been approved in the US and EU for the treatment of patients with hereditary antithrombin deficiency,<sup>13,14</sup> and plant cell-expressed recombinant glucocerebrosidase (ELELYSO<sup>®</sup>) has been approved for the treatment of patients with Gaucher disease in the US.<sup>15,16</sup> Although mAbs produced by transgenic animals or transgenic plants have not been approved for therapeutic

© Minoru Tada, Ken-ichiro Tatematsu, Akiko Ishii-Watabe, Akira Harazono, Daisuke Takakura, Noritaka Hashii, Hideki Sezutsu, and Nana Kawasaki

\*Correspondence to: Minoru Tada; Email: m-tada@nihs.go.jp

Submitted: 03/19/2015; Revised: 07/20/2015; Accepted: 07/22/2015

<http://dx.doi.org/10.1080/19420862.2015.1078054>

This is an Open Access article distributed under the terms of the Creative Commons Attribution-Non-Commercial License (<http://creativecommons.org/licenses/by-nc/3.0/>), which permits unrestricted non-commercial use, distribution, and reproduction in any medium, provided the original work is properly cited. The moral rights of the named author(s) have been asserted.

application, recombinant mAbs have been produced by using transgenic animal (goat<sup>17</sup> and chicken<sup>18</sup>) or transgenic plant (tobacco,<sup>11,19,20</sup> moss<sup>21-23</sup> and duckweed<sup>24</sup>) expression systems.

The silkworm (*Bombyx mori*) is a highly domesticated insect that has been widely used as an experimental animal model in academic research.<sup>25</sup> The silkworm has also been applied to the production of recombinant proteins.<sup>26-29</sup> Transient expression systems with baculovirus-infected silkworms have been used for the production of recombinant proteins,<sup>27,29</sup> and both recombinant canine interferon gamma and feline interferon gamma produced by baculovirus-infected silkworms have already been approved as veterinary drugs.<sup>30,31</sup> Further, the development of a system for stable germline transformation using *piggyBac* transposon-derived vectors enables the mass production of recombinant proteins in transgenic silkworms.<sup>32</sup> Silkworms can produce large amounts of silk proteins (0.2~0.5 g / worm), and their speed of protein biosynthesis is considered to be 10<sup>6</sup>-fold greater than that in mammalian culture cells.<sup>33</sup> Various proteins have been successfully produced in the silk glands of transgenic silkworms,<sup>34-37</sup> and improvements to these production systems are in progress.<sup>38</sup> The life span of silkworm from eggs to adult moths is approximately 6–7 weeks and one female moth lays 200 to 500 eggs. The cost of silkworm rearing is less than 5 cents per larva, and it takes approximately 60 d to generate transgenic silkworms. Because of their cost-effective breeding and relatively easy production scale-up, transgenic silkworms show promise as a novel production system for mAbs and other biopharmaceuticals. However, the effects of the post-translational modifications, including N-linked glycosylation, on the biological activities of mAbs produced in silkworms have been poorly understood.

In this study, in order to assess the usefulness of transgenic silkworms for the production of therapeutic mAbs, we generated a transgenic silkworm expressing a human-mouse chimeric anti-CD20 mAb, and compared the biological activities between this mAb and the anti-CD20 mAb produced by CHO cells (MabThera®). Anti-CD20 mAbs produced in transgenic silkworms showed an antigen-binding property similar to that of MabThera, but exhibited a stronger antibody-dependent cell-mediated cytotoxicity (ADCC) and weaker complement-dependent cytotoxicity (CDC) than MabThera. Post-translational modification analysis revealed that these biological properties were attributable to the characteristic N-glycan structures (lack of core-fucose and galactose at the non-reducing terminal).

## Results

### Generation of transgenic silkworms expressing an anti-CD20 monoclonal antibody

To establish transgenic silkworm strains expressing an anti-CD20 mAb H chain or L chain, we constructed 2 vectors, pBac [UAS\_antiCD20 mAb HC/3 × P3-EYFP] and pBac [UAS\_antiCD20 mAb LC/3 × P3-AmCyan] (Fig. 1), and separately injected these plasmids into silkworm eggs with helper plasmid DNA and mRNA that supply the *piggyBac* transposase (Fig. S1). The former plasmid encoded the anti-CD20 mAb H chain gene

under control of a UAS promoter; and the latter plasmid encoded the anti-CD20 mAb L chain gene. These two plasmids were separately injected into silkworm eggs, and G0 adults were mated with other G0 adults potentially carrying the same plasmid to generate G1 eggs. G1 embryos were screened for expressions of EYFP or AmCyan gene in the eyes. Two lines for the anti-CD20 mAb H chain and 4 lines for the anti-CD20 mAb L chain were obtained (Table S1). To express each gene in the middle silk glands (MSGs) of transgenic silkworms, silkworms from each line were mated with Ser1-GAL4 strain<sup>38</sup> (Fig. 1) that expresses the GAL4 gene in MSGs. In the next generation, the transgenic silkworms that expressed both EYFP and DsRed2 in embryonic eyes were selected to generate anti-CD20 mAb H chain-expressing lines (H lines), and those that expressed both AmCyan and DsRed2 were selected to generate anti-CD20 mAb L chain-expressing lines (L lines). To confirm the expression of these genes in MSGs, the lysates extracted from MSGs of the H lines or L lines were analyzed via sodium dodecyl sulfate-polyacrylamide gel electrophoresis (SDS-PAGE) and western blotting (Fig. 2A). Specific bands of approximately 50 kDa and 25 kDa were evident in the H line lanes or L line lanes, respectively, but not in the negative control lanes on western blots. The H line No. 1 and L line No. 2, which showed the highest levels of expression, were used in the subsequent experiments.

To express both the anti-CD20 mAb H chain and L chain in one larva, the H line and the L line were mated with each other (H+L line) and transgenic silkworms that expressed EYFP, AmCyan, and DsRed2 in the eyes were selected (H+L line). To confirm the expression and the assembly of the anti-CD20 mAb H chain and L chain, the lysates extracted from MSGs and cocoons of the H+L line were analyzed by SDS-PAGE and western blotting under reducing conditions and also separately under non-reducing conditions (Fig. 2B). Under reducing conditions, the specific 50 kDa and 25 kDa bands were detected in the H+L line lanes derived from either MSGs or cocoons on CBB-stained gels and western blot. In contrast, under non-reducing conditions, in each lane containing MSG or cocoon lysate, a band of approximately 150 kDa was evident in CBB-stained gels, and an intense band of 150 kDa and several additional weak bands were detected on western blot. These results suggested that most of the anti-CD20 mAb H chain and L chain molecules expressed in MSGs were assembled to H<sub>2</sub>L<sub>2</sub>-subunit structures and secreted into the sericin layer of cocoons.

### Anti-CD20 mAbs derived from transgenic silkworms showed CD20-binding properties similar to that of MabThera

To estimate the biological properties of anti-CD20 mAbs derived from transgenic silkworms, we purified anti-CD20 mAbs from the lysates of MSGs or cocoons derived from transgenic silkworms by affinity chromatography using a protein G column (Fig. 3A). Yield of mAbs derived from MSGs and cocoons was 600 and 250 μg per worm, respectively. Both the mAbs ran on the gel at similar molecular weight (Fig. 3B). Purity of mAbs derived from transgenic silkworms is more than 95% when calculated by densitometer analysis of CBB-stained gel, and protein aggregates were hardly detected by dynamic light scattering

analysis (data not shown). We then examined the CD20-binding properties of the mAbs by flow cytometric analysis. As shown in **Figure 4A and B**, both MabThera and the anti-CD20 mAbs derived from transgenic silkworms exhibited binding to Daudi, a human Burkitt's lymphoma cell line that strongly expresses CD20, with a similar dose-response relationship. These results suggest that the anti-CD20 mAbs were correctly expressed and folded in the MSGs of transgenic silkworms and possessed their antigen-binding properties.

### Comparison of the binding affinity to human Fc receptors between anti-CD20 mAbs derived from transgenic silkworms and MabThera

The interaction between FcγRs and the Fc region of mAbs plays an important role in the effector functions of mAbs.<sup>39</sup> Among the human FcγRs, FcγRIIIa is the only activating FcγR expressed in natural killer (NK) cells, and is involved in the ADCC by tumor-targeting mAbs. To assess the FcγR-binding affinity of anti-CD20 mAbs derived from transgenic silkworms, we performed surface plasmon resonance (SPR) analysis using the recombinant extracellular domain of human FcγRIIIa and that of FcγRI, a high-affinity human Fc receptor, as a control. The anti-CD20 mAbs derived from transgenic silkworms showed slightly weaker binding to human FcγRI than did MabThera (the  $K_D$  values of MabThera, MSG-derived mAbs and cocoon-derived mAbs were  $2.08 \pm 0.01$ ,  $2.49 \pm 0.01$  and  $2.52 \pm 0.03$  nM, respectively) (**Fig. 5A, B** and **Table 1**). On the other hand, the anti-CD20 mAbs derived from transgenic silkworms showed 4-fold stronger binding affinity to FcγRIIIa than did MabThera (the  $K_D$  values of MabThera, MSG-derived mAbs and cocoon-derived mAbs were  $92.2 \pm 1.08$ ,  $23.1 \pm 0.06$ , and  $24.9 \pm 0.45$  nM, respectively) (**Fig. 5A, B** and **Table 1**).

The neonatal Fc receptor (FcRn) is known to regulate the serum half-lives of IgG.<sup>40,41</sup> FcRn binds to the Fc domain of IgG at acidic pH, but not at neutral pH; therefore, FcRn protects IgGs against degradation in the lysosomes and recycles them by releasing into plasma. The FcRn-binding affinity of mAbs at acidic pH is known to be correlated with the serum half-lives of mAbs.<sup>42</sup> As shown in **Figure 5**, the anti-CD20 mAbs derived from transgenic silkworms showed slightly weaker binding to human FcRn than did MabThera (the  $K_D$  values of MabThera, MSG-derived mAbs and cocoon-derived mAbs were  $299 \pm 17$ ,  $420 \pm 19$  and  $404 \pm 26$  nM, respectively).

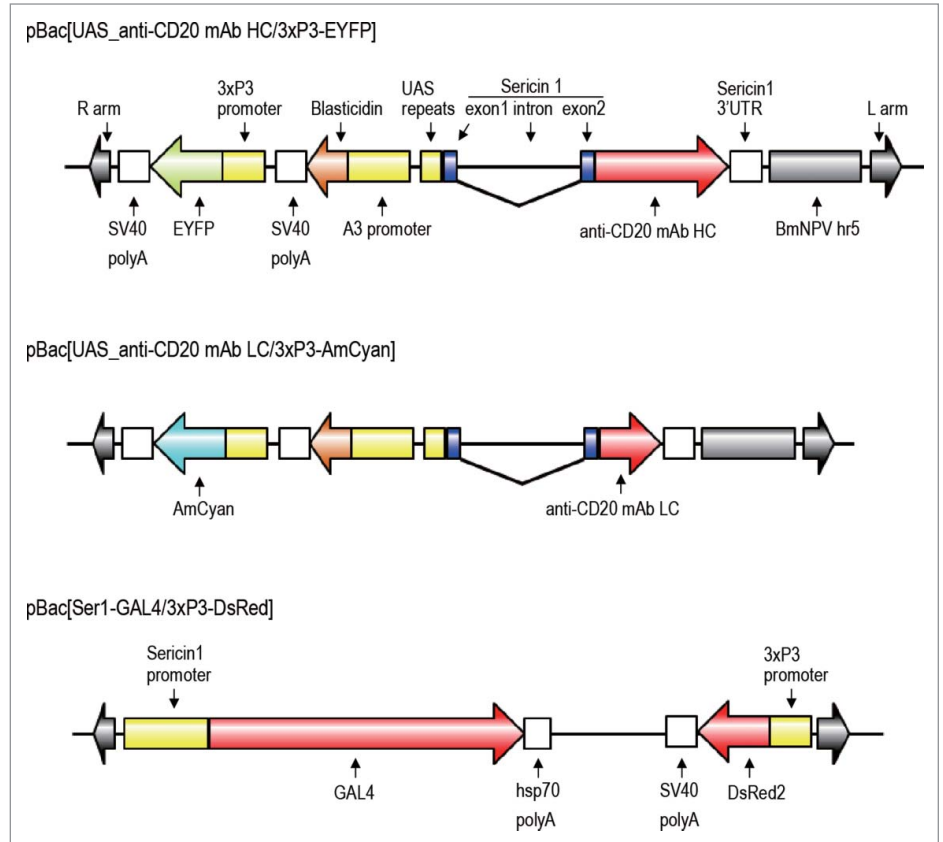


**Figure 1.** Structures of the plasmids used to generate transgenic silkworms. Each plasmid has right and left arms of *piggyBac* and the 3 × P3-fluorescent gene cassette for a screening marker (EYFP, AmCyan, or DsRed2). Plasmids pBac[UAS\_anti-CD20 mAb HC/3 × P3-EYFP] and pBac[UAS\_anti-CD20 mAb LC/3 × P3-AmCyan] encode the anti-CD20 mAb H chain gene and the anti-CD20 mAb L chain gene, respectively, under the control of a UAS promoter, and contain a BmNPV-derived hr5 enhancer and an A3-Blasticidin cassette. The anti-CD20 H and L genes were fused to the signal peptide sequence of the sericin 1 gene encoded by exon 1 and 18 bp of exon 2. The plasmid pBac[Ser1-GAL4/3 × P3-DsRed] encodes the GAL4 gene under the control of the sericin1 promoter.

### Effector functions of anti-CD20 mAbs derived from transgenic silkworms

We next compared the biological activities of anti-CD20 mAbs derived from transgenic silkworms with those of MabThera. MabThera exerts cytotoxic activities against CD20-overexpressing B-cell lymphomas by immune-mediated effector functions including ADCC and CDC.<sup>43</sup> Because the activation of FcγRIIIa by antigen-bound mAbs is an important step in NK cell-mediated ADCC activity, we first examined the activation of FcγRIIIa by anti-CD20 mAbs by using Jurkat/FcγRIIIa/NFAT-Luc reporter cells, in which luciferase expression was induced by the activation of FcγRIIIa.<sup>44</sup> When Daudi and Jurkat/FcγRIIIa/NFAT-Luc reporter cells were co-cultured in the presence of MabThera, an increase in the activation of FcγRIIIa was observed in a dose-dependent manner (the  $EC_{50}$  was 113 pM). Under this condition, the anti-CD20 mAbs derived from transgenic silkworms activated FcγRIIIa more strongly than MabThera (the  $EC_{50}$  values of the MSG- and the cocoon-derived mAbs were 17.5 and 20.3 pM, respectively) (**Fig. 6A**),

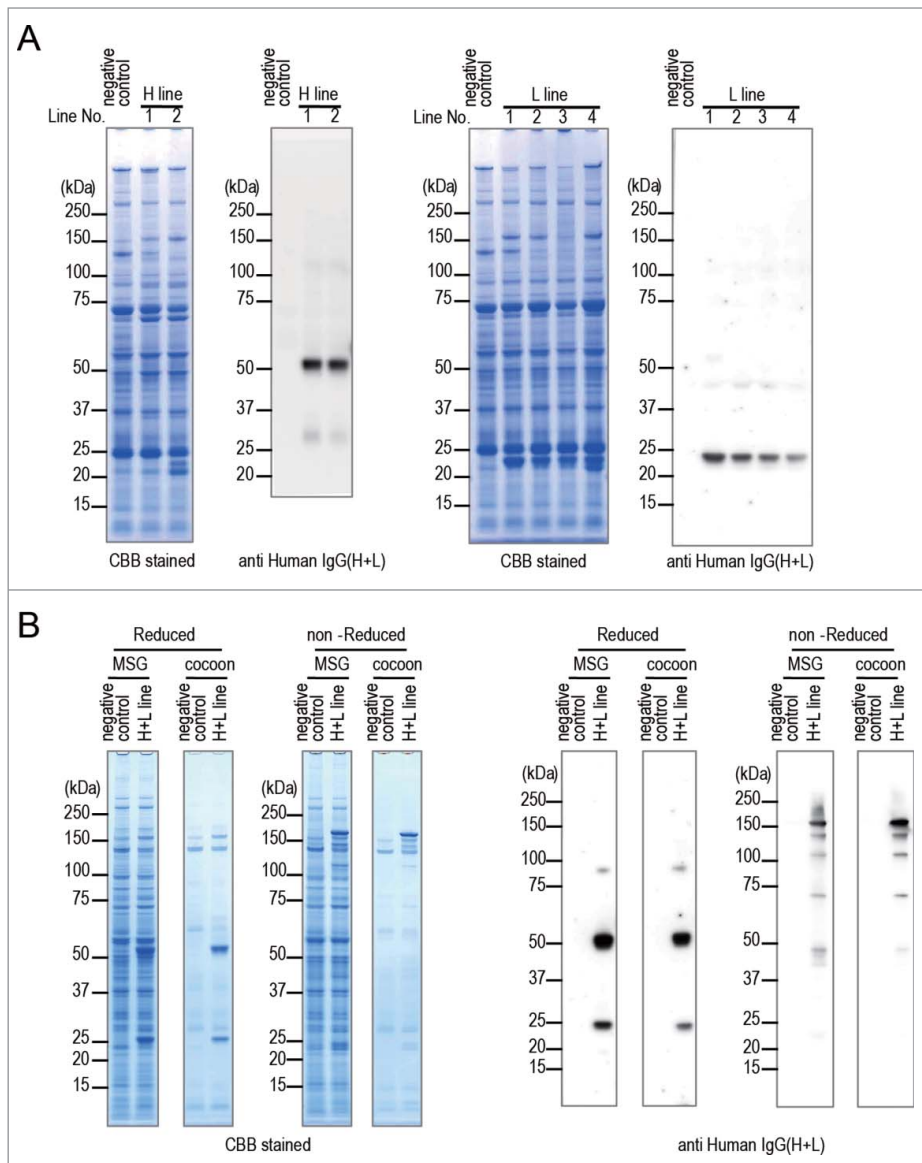


**Figure 2.** Expression of anti-CD20 mAb in transgenic silkworms. **(A)** The protein lysates extracted from MSGs of H line or L line transgenic silkworms were separated by SDS-PAGE followed by staining with CBB or by western blotting with an anti-Human IgG(H<sup>+</sup>L) antibody. The protein lysates extracted from MSGs of transgenic silkworms that harbored only the Ser1-GAL4 construct were used as negative controls. The numbers above the gels or western blots indicate the line number of each transgenic strain. **(B)** The protein lysates extracted from MSGs or cocoons of the H<sup>+</sup>L line transgenic silkworms were separated by SDS-PAGE under reducing or non-reducing conditions. Gels were stained with CBB or subjected to protein gel blotting using an anti-Human IgG(H<sup>+</sup>L) antibody. The lysates obtained from the transgenic silkworms harboring only the Ser1-GAL4 construct were used as a negative control.

suggesting that the anti-CD20 mAbs derived from transgenic silkworms may exhibit a stronger ADCC activity than MabThera. Next, we performed an ADCC assay using human peripheral blood mononuclear cells (PBMCs) as effector cells. As shown in **Figure 6B**, the anti-CD20 mAbs derived from transgenic silkworms showed stronger ADCC activity against Daudi cells than did MabThera (the EC<sub>50</sub> values for MabThera, MSG-derived mAbs and cocoon-derived mAbs were 303, 45.9 and 26.7 pM, respectively).

CDC is one of the important mechanisms of action for the tumor-killing activity of MabThera. When Daudi cells were cocultured with MabThera in the presence of human serum, cell lysis was observed in a dose-dependent manner (**Fig. 7**). In contrast to ADCC, the CDC caused by anti-CD20 mAbs derived from transgenic silkworms was significantly weaker than that caused by MabThera ( $p < 0.01$  at 3  $\mu\text{g/ml}$ , and  $p < 0.001$  at 10  $\mu\text{g/ml}$ ) (**Fig. 7**). These results suggest that anti-CD20 mAbs derived from transgenic silkworms exhibit different effector functions than MabThera produced in CHO cells.

#### Fc glycosylation analysis of anti-CD20 mAbs derived from transgenic silkworms

To reveal the quality attributes characterizing the unique biological activities of anti-CD20 mAbs produced in transgenic silkworms, we next performed peptide mapping by liquid chromatography/mass spectrometry (LC/MS). There was a significant difference in N-glycosylation profile between the CHO- and the silkworm-derived mAbs, but not in other post-translational modifications including oxidation and deamidation (data not shown). LC/MS data of the mAbs tryptic digest showed that MabThera contained mainly core-fucosylated biantennary complex-type N-glycans (the % peak areas of agalactosylated, core-fucosylated biantennary N-glycan (A2G0F), monogalactosylated, core-fucosylated biantennary N-glycan (A2G1F) and digalactosylated, core-fucosylated biantennary N-glycan (A2G2F) were 62.2, 27.0 and 2.2, respectively) (**Fig. 8**). In contrast, the N-glycans attached to anti-CD20 mAbs derived from transgenic

silkworms were mostly afucosylated, and agalactosylated mono-antennary N-glycan (A1G0), Man-5 and agalactosylated biantennary N-glycan (A2G0) were the major N-glycans (the % peak areas of A1G0, Man-5 and A2G0 were 48.8, 26.4 and 10.0 in MSG-derived mAbs, and 43.8, 31.0 and 10.9 in cocoon-derived mAbs, respectively) (**Fig. 8**). Only a small amount of fucosylated N-glycans were detected in the transgenic silkworm-derived mAbs. Next, we performed a linkage analysis of the fucosylated N-glycans detected in anti-CD20 mAbs derived from transgenic



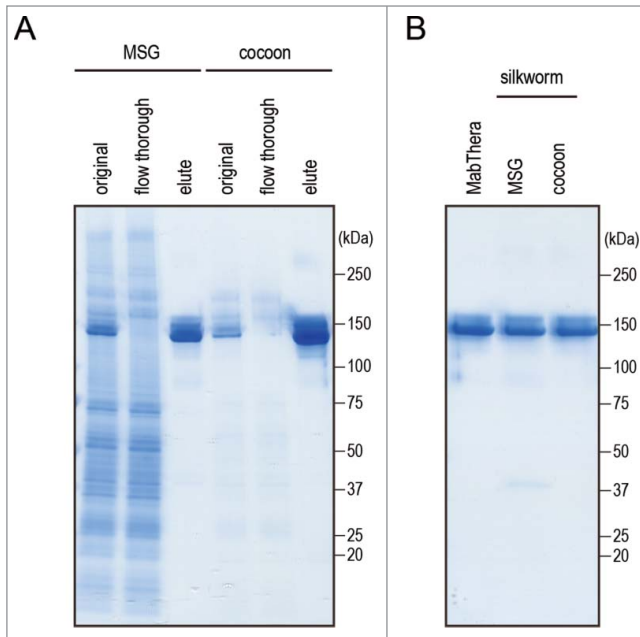


**Figure 3.** Purification of anti-CD20 mAbs from the transgenic silkworms. **(A)** Anti-CD20 mAbs were purified from the lysates of MSGs or cocoons derived from transgenic silkworms by affinity chromatography using a Protein G column. The lysates (original), flow-through fractions from the Protein G column, and eluted fractions were analyzed by non-reducing SDS-PAGE. **(B)** MabThera and anti-CD20 mAbs derived from transgenic silkworms showed the same migration pattern on non-reducing SDS-PAGE.

silkworms. When the transgenic silkworm-derived mAbs were treated with peptide N-glycosidase F, which cleaves all N-glycans from glycoproteins unless the core *N*-acetylglucosamine residue is  $\alpha$ 1,3-fucosylated, the mass chromatogram of the glycopeptide

was completely abolished (data not shown), suggesting that the fucosylated N-glycans detected in transgenic silkworm-derived mAbs were  $\alpha$ 1,6-fucosylated.

## Discussion

The selection of appropriate cells to be used for production is a crucial step in the development of biopharmaceuticals, and thus a detailed understanding of the characteristics of the production cells is indispensable. Among the various post-translational modifications occurring in biopharmaceuticals, N-linked glycosylation is well known to differ according to the cells chosen for production, and the N-glycan structures are correlated with the biological properties of some biopharmaceuticals.<sup>45-47</sup> In human IgG1, Asn-297 (EU numbering) in the CH2 domain is a conserved N-glycosylation site. The major glycans attached to Asn-297 are core-fucosylated biantennary complex-type glycans,<sup>48</sup> and the correlations between the N-glycan structure in Asn-297 and the effector functions of mAbs have been well elucidated;<sup>49,50</sup> the absence of  $\alpha$ 1,6-fucose residue attached to the core *N*-acetylglucosamine residue enhances the binding of mAbs to Fc $\gamma$ RIIIa and the ADCC activity,<sup>51,52</sup> and galactose residues at the non-reducing terminals are correlated with the binding to complement C1q and CDC activity.<sup>53-55</sup> Therefore, the N-glycan structure in Asn-297 is one of the critical quality attributes in therapeutics mAbs that use these effector functions as part of their mechanism of action.

In this study, we developed a transgenic silkworm that stably expresses human-mouse chimeric anti-CD20 mAbs. Anti-CD20 mAbs derived from the transgenic silkworm showed similar CD20-binding properties compared to MabThera produced by CHO cells, but exhibited stronger ADCC and weaker CDC activity than MabThera. These differences in the effector functions could be explained by the N-glycan structure at the Fc region (Asn-297). Namely, most of the N-glycans attached to transgenic silkworm-derived mAbs were afucosylated species, resulting in the enhancement of the Fc $\gamma$ RIIIa-binding affinity and ADCC activity. In addition, the absence of galactose residues at the non-reducing terminal may have contributed to the diminished CDC activity in the transgenic silkworm-derived mAbs. To date, several researchers have reported on the expression of mouse or human IgGs in silkworms, and have analyzed their insect-specific N-glycan structures,<sup>37,56,57</sup> but the influences of their N-glycan structures on the effector functions, including ADCC and CDC activity, have remained uncertain. This is the first report demonstrating the distinctive effector functions of the mAbs

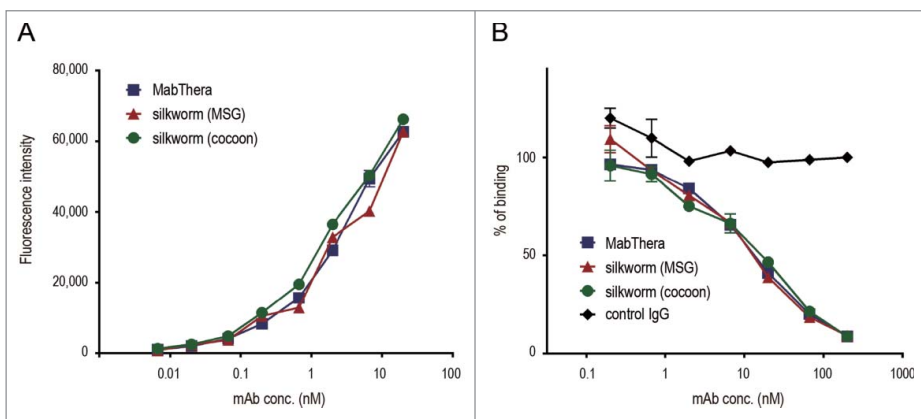


**Figure 4.** CD20-binding properties. **(A)** Daudi cells were incubated with anti-CD20 mAbs and their binding properties were assessed by flow cytometric analysis using Alexa488-conjugated F(ab')<sub>2</sub> anti-human IgG Fc. The mean fluorescence intensities were plotted against the mAbs concentration ( $n = 3$ , bars indicate SEM). **(B)** Daudi cells were incubated with DyLight 488-labeled MabThera and serially diluted unlabeled mAbs. Percentages of DyLight 488-labeled MabThera binding were calculated by the mean fluorescence intensities and plotted against the unlabeled mAbs concentration ( $n = 3$ , bars indicate SEM).

produced by silkworms, and the results indicate that the transgenic silkworms would be useful for the production of tumor-targeting mAbs with higher ADCC activity. Although CDC activity is one of the mechanisms of action of anti-CD20 mAbs, complement activation also plays a role in antibody-induced infusion reactions.<sup>58,59</sup> Therefore, mAbs with increased ADCC activity but reduced CDC activity may hold promise as therapeutics with lesser adverse reactions.

N-glycosylation sometimes influences the pharmacokinetics of biopharmaceuticals.<sup>46</sup> For example, the sialic acid content of erythropoietin is closely related to the serum clearance,<sup>60-62</sup> and mannose 6-phosphate in some lysosome enzymes is needed for the targeting to lysosomes.<sup>63,64</sup> Because silkworm and most insects lack the biosynthetic pathway needed to produce these N-glycan structures,<sup>65,66</sup> glyco-engineering technologies are indispensable for the production of these biopharmaceuticals.

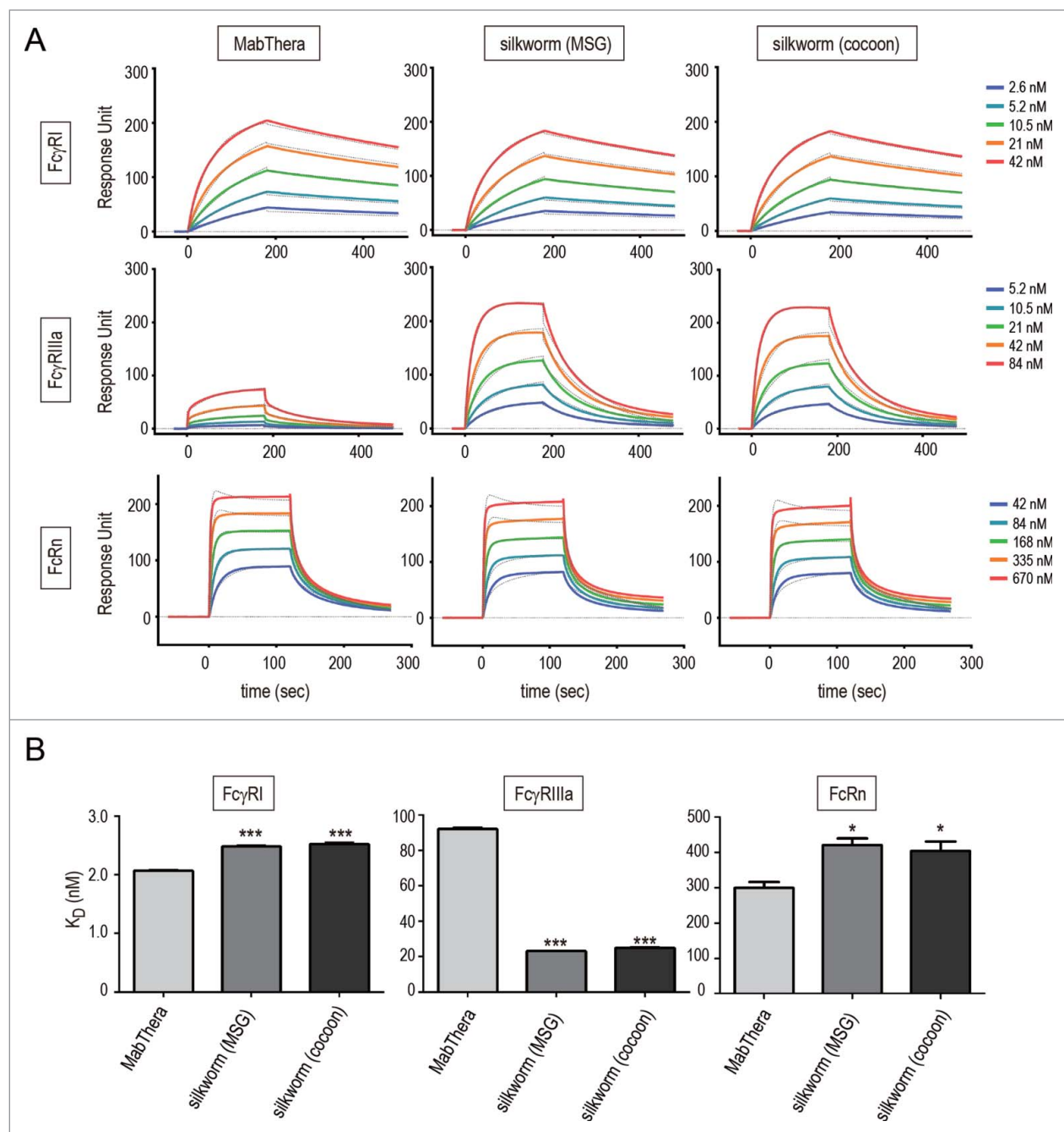


**Figure 5.** Binding affinity to human Fc receptors. Binding affinities of anti-CD20 mAbs to Fc $\gamma$ RI, Fc $\gamma$ RIIIa and FcRn were measured by an SPR analysis. (A) Binding sensorgrams corrected for both the surface blank and the buffer injection control are represented. Dashed lines indicate the fitting curves generated by 1:1 binding model for Fc $\gamma$ Rs and bivalent model for FcRn, respectively. (B) Dissociation constant ( $K_D$ ) values are represented as mean + SD (n = 3). \*, p < 0.05; \*\*, p < 0.01; \*\*\*, p < 0.001.

**Table 1.** Binding affinities to human Fc receptors

<b>Fc<math>\gamma</math>RI (1:1 binding model)</b>					
	$k_a$ (1/Ms)		$k_d$ (1/s)		$K_D$ (M)
MabThera	$4.34 \times 10^5$		$9.01 \times 10^{-4}$		$2.07 \pm 0.01 \times 10^{-9}$
silkworm (MSG)	$3.73 \times 10^5$		$9.30 \times 10^{-4}$		$2.49 \pm 0.01 \times 10^{-9}$
silkworm (cocoon)	$3.79 \times 10^5$		$9.38 \times 10^{-4}$		$2.52 \pm 0.03 \times 10^{-9}$
<b>Fc<math>\gamma</math>RIIIa (1:1 binding model)</b>					
	$k_a$ (1/Ms)		$k_d$ (1/s)		$K_D$ (M)
MabThera	$7.67 \times 10^4$		$7.13 \times 10^{-3}$		$9.22 \pm 0.10 \times 10^{-8}$
silkworm (MSG)	$4.05 \times 10^5$		$9.33 \times 10^{-3}$		$2.31 \pm 0.01 \times 10^{-8}$
silkworm (cocoon)	$4.05 \times 10^5$		$9.89 \times 10^{-3}$		$2.49 \pm 0.04 \times 10^{-8}$
<b>FcRn (bivalent model)</b>					
	$k_{a1}$ (1/Ms)	$k_{d1}$ (1/s)	$k_{a2}$ (1/Ms)	$k_{d2}$ (1/s)	$K_D$ (M)
MabThera	$3.15 \times 10^5$	$9.43 \times 10^{-2}$	$1.53 \times 10^{-4}$	$8.77 \times 10^{-3}$	$2.99 \pm 0.17 \times 10^{-7}$
silkworm (MSG)	$2.91 \times 10^5$	$1.23 \times 10^{-1}$	$1.13 \times 10^{-4}$	$5.71 \times 10^{-3}$	$4.21 \pm 0.19 \times 10^{-7}$
silkworm (cocoon)	$2.92 \times 10^5$	$1.19 \times 10^{-1}$	$1.25 \times 10^{-4}$	$6.08 \times 10^{-3}$	$4.04 \pm 0.26 \times 10^{-7}$

The effects of the N-glycan structures at Asn-297 in mAbs on the pharmacokinetics have remained a matter of controversy. As described above, FcRn is a critical regulator of the serum half-lives of mAbs. Previous comparisons between several glyco-engineered variants, including aglycosylated mAbs and mAbs with afucosylated or high mannose-type N-glycans have revealed that N-glycan structures at Asn-297 did not influence the FcRn-binding properties.<sup>67,68</sup> On the other hand, it has been reported that the mAbs with high mannose-type N-glycan showed faster serum clearance than the mAbs with complex-type N-glycan.<sup>68-70</sup> Although the detailed mechanism of the accelerated serum clearance of mAbs with high mannose-type glycan is unclear, the content of high mannose-type glycan is considered to be one of the important quality attributes of therapeutic mAbs. In this study, we revealed that anti-CD20 mAbs derived from transgenic silkworms contained ~30% of high mannose-type glycan (M5, M6 and M7) (Fig. 8), and their binding affinities to FcRn were slightly weaker than that of MabThera (Fig. 5). Although this slight difference in FcRn-binding affinity might be expected to have no effect on the pharmacokinetic profiles of mAbs, the presence of high mannose-type glycan may influence to their serum half-lives. Further pharmacokinetic studies will thus be needed for the pharmaceutical development of mAbs derived from transgenic silkworms.

Recombinant proteins produced in non-human cells often have N-glycans not present in the human body, and these have the potential to induce immunogenic reactions when administered in humans.<sup>71</sup> Both  $\alpha$ 1,3- and  $\alpha$ 1,6-fucose residues attached to the core N-acetylglucosamine residue are found in insect N-glycans. The  $\alpha$ 1,3 core fucose is not present in the N-glycans of human proteins, and this fucose has the potential to induce immunogenic reactions. Iizuka et al. previously reported that core-fucosylated N-glycans were attached to the proteins present in the fat bodies but not in the cocoons and MSGs of silkworms, and they also revealed that the N-glycans attached to murine

mAbs expressed in the cocoons contained no detectable core-fucose residues.<sup>37</sup> In our experiment, only a small amount of core-fucosylated N-glycans was detected in the anti-CD20 mAbs derived from MSGs and cocoons (1.1% and 3.5%, respectively), but these were  $\alpha$ 1,6-fucosylated. These results suggest that mAbs produced in the MSGs and cocoons of transgenic silkworms do not contain  $\alpha$ 1,3 core fucose, and may thus have therapeutic application without the induction of immunogenic reactions.

In conclusion, anti-CD20 mAbs produced in transgenic silkworms showed an antigen-binding property similar to that of MabThera, but exhibited stronger ADCC and weaker CDC than MabThera. Post-translational modification analysis revealed that these biological properties were attributable to the characteristic N-glycan structures (lack of core-fucose and galactose at the non-reducing terminal). These results indicate that transgenic silkworms may be a promising expression system for tumor-targeting mAbs with higher cytotoxic activity. It must be noted that, for clinical use of mAbs produced by transgenic silkworms, there are some problems to be solved. These include mass scale production of mAbs, development of the banking system for transgenic silkworms, and control of process-related impurities. We are now trying to improve protein expression level by modifying the expression vectors, and we have started to establish the banking system of transgenic silkworms by using frozen ovary and sperm. Although there is no guidance or guideline specific for transgenic silkworm-derived products, the experiences of mammalian cells or transgenic animal-derived biopharmaceuticals are useful for the quality control of transgenic silkworm-derived products.

## Materials and Methods

### Construction of expression vectors

Plasmids for generating transgenic silkworms expressing the anti-CD20 mAb H chain or L chain are shown in Figure 1 and

**Table 2.** Primers used in this study

Name	Sequence
Primer	
hr5 U	5'-CGATAAGCTTACTAGCCTTTGTCATTGCTTGATTG-3'
hr5 L	5'-CTAGTGATTCCATAACGTCCTGTCGATTCAACGTA-3'
A3pro U	5'-GGATCCTAGGTGCGCGTTACCATATATG-3'
A3pro L	5'-GATATCCATGGTCTTGAATTAGTCTGCAAG-3'
SV40polyA U	5'-GATATCAGATCTCATAATCAGCCATACCA-3'
SV40polyA L	5'-GTCGACCTAGGATACATTGATGAGTTTGG-3'
Sersig U	5'-CCATGGAAATCAAATGCGTTTCGTTCTGT-3'
SigBlaOE L	5'-CAAAGGCTTGGCCATGTGGTGACCGAAAGC-3'
SigBlaOE U	5'-GCTTTCGGTCAACACATGGCCAAGCCTTTG-3'
Bla L	5'-AGATCTCCCGGGACGTGCAGTCTGCTCC-3'
SerTATASerK U	5'-CTGCAGGCATGCAAGCTTGAGCTCGACCGC-3'
SerTATASerKOE L	5'-CACAGAACGAAACGCATGTTGGCGGTCTTT-3'
SerTATASerKOE U	5'-AAAGACCGCAACATGCGTTTCGTTCTGTG-3'
Sersig L	5'-GCCTAGGGAGACGGCAGATCGTCTCCAG CTTTTACGCTGAGCGC-3'
EYFP U	5'-CCATGGAAATCAAATGGTGGAGCAAGGGCG-3'
EYFP L	5'-GCGGCCGCTTATCTAGATCCGGTGGATCCCGG-3'
AmCyan U	5'-CCATGGAAATCAAATGGCCCTGTCCAACA-3'
AmCyan L	5'-GCGGCCGCTCAGAAGGGCACCACGGAGGTGAT-3'
Rituximab HC U	5'-GCGTCTCAAGCTCAGTACAACCTGCAGCAG-3'
Rituximab HC L	5'-GCGTCTCCCTAGTCAATTTACCCGGAGACAG-3'
Rituximab LC U	5'-GCGTCTCAAGCTCAAATGTTCTCTCCAG-3'
Rituximab LC L	5'-GCGTCTCCCTAGTCAACACTCTCCCTGTT-3'
adapter	
PstI adapter	5'-CAGATCTGCTAGCCTCGAGCTGCA-3' 3'-ACGTGTCTAGACGATCGGAGCTCG-5'

were prepared as follows. To invert the direction of the 3 × P3-EGFP cassette, the EcoRI fragment of pBac[SerUAS/3×P3-EGFP],<sup>38</sup> which contains a 3×P3-EGFP cassette, was excised and re-inserted in the opposite direction of that in the original plasmid, yielding pBac[SerUAS/3×P3-EGFPinv]. The BmNPV (Bombyx mori nuclear polyhedrosis virus)-derived *hr5* enhancer sequence amplified from pGEM-hr5 (kindly provided by Dr. H. Bando, Hokkaido University) with primers hr5 U and hr5 L (Table 2) was inserted into the EcoRV site of pBac[SerUAS/3×P3-EGFPinv]; the PstI adapter (Table 2) was then inserted into the PstI site of the resultant plasmid to generate pBac[SerUAS-hr5/3×P3-EGFPinv]. Simultaneously, an A3-Blasticidin cassette was generated as an auxiliary screening marker. The A3 promoter sequence amplified from pBacA3GAL4/3×P3DsRed<sup>72</sup> with primers A3pro U and A3pro L (Table 2) was digested with BamHI and EcoRV and inserted into the BamHI – EcoRV site of pBluescriptII SK (–) vector to generate A3 promoter/pBS. The SV40 polyA sequence amplified from pBacA3GAL4/3×P3DsRed with primers SV40polyA U and SV40polyA L (Table 2) was digested with EcoRV and SalI and then inserted into the EcoRV-SalI site of A3 promoter/pBS; this process yielded A3pro-SV40/pBS.

To add the signal peptide sequence of the sericin 1 gene to the Blasticidin gene, overlap-extension PCR (OE PCR) was performed with pBac[UAS-ser\_sig-EGFP/3×P3-EGFP]<sup>38</sup> and pIB/V5-His (Life Technologies) as templates, and Sersig U, SigBlaOE L, SigBlaOE U, and Bla L (Table 2) as primers. The NcoI-BglII fragment of this PCR product was inserted into the NcoI-BglII site of A3pro-SV40/pBS, and the resultant plasmid was

designated A3pro-Bla-SV40/pBS. The BamHI-XhoI fragment of A3pro-Bla-SV40/pBS was inserted into the BglII-XhoI site of pBac[SerUAS\_hr5/3×P3-EGFPinv] to generate pBac[SerUAS\_hr5/3×P3-EGFPinv\_A3-Bla]. The exon-intron sequence of the sericin1 gene, which contains a TATA sequence and a signal peptide sequence, was amplified by OE PCR from a pBac[SerUAS-ser\_int-EGFP/3×P3-EGFP] template with SerTATASerK U, SerTATASerKOE L, SerTATASerKOE U, and Sersig L (Table 2) as primers. The SnaBI-BlnI fragment of this OE PCR product was inserted into the SnaBI-BlnI site of pBac[SerUAS\_hr5/3×P3-EGFPinv\_A3-Bla], yielding pBac[SerUAS\_Ser1intron\_hr5/3×P3-EGFPinv\_A3-Bla].

To change the fluorescent marker gene, the EYFP gene was amplified from the pEYFP-N1 (Takara) with the EYFP U and EYFP L primers (Table 2); similarly, the AmCyan gene was amplified from the pAmCyan1-N1 (Takara) with the AmCyan U and AmCyan L primers (Table 2). The NcoI-NotI fragment from each of these PCR products was inserted into the NcoI-NotI site of pBac[SerUAS\_Ser1intron\_hr5/3×P3-EGFPinv\_A3-Bla]; these processes generated 2 plasmids, pBac[SerUAS\_Ser1intron\_hr5/3×P3-EYFP\_A3-Bla] and pBac[SerUAS\_Ser1intron\_hr5/3×P3-AmCyan\_A3-Bla]. The anti-CD20 mAb H chain gene was amplified from pFUSE\_Rituximab HC with primers anti-CD20 mAb HC U and anti-CD20 mAb HC L (Table 2); the BsmBI fragment of this PCR product was inserted into the BsmBI site of pBac[SerUAS\_Ser1intron\_hr5/3×P3-EYFP\_A3-Bla] to generate pBac[UAS\_antiCD20 mAb HC/3×P3-EYFP]. The anti-CD20 mAb L chain gene was amplified from pFUSE2\_Rituximab LC with primers anti-CD20 mAb LC U and anti-CD20 mAb LC L (Table 2); the BsmBI fragment of this PCR product was inserted into the BsmBI site of pBac[SerUAS\_Ser1intron\_hr5/3×P3-AmCyan\_A3-Bla] to generate pBac[UAS\_antiCD20 mAb LC/3×P3-AmCyan].

#### Generation of transgenic silkworms expressing the H chain or L chain of anti-CD20 mAb

The silkworm strain w1-pnd, which produces non-dia-pausing silkworms, non-pigmented eggs, and non-pigmented eyes, was used to generate transgenic silkworms. The dia-pausing strain w-1 was then used to maintain each transgenic strain. These strains were maintained at the Transgenic Silkworm Research Unit, National Institute of Agrobiological Sciences. Silkworm larvae were reared on an artificial diet (Nosan, Yokohama, Japan) at 25°C. Transgenic silkworms were generated as previously reported using the plasmid pBac[UAS\_antiCD20 mAb HC/3 × P3-EYFP] and pBac[UAS\_antiCD20 mAb LC/3 × P3-AmCyan] as vectors (Fig. S1).<sup>32,73</sup>

pBac[UAS\_antiCD20 mAb HC/3×P3-EYFP] and pBac[UAS\_antiCD20 mAb LC/3 × P3-AmCyan] were separately injected into eggs with helper plasmid DNA and mRNA that express the *piggyBac* transposase gene, and G0 adults were mated with other G0 adults that might carry the same transgenic construct. The G1 silkworms were screened during the late embryonic stage for the expression of EYFP or AmCyan driven by the 3 × P3 promoter in the embryonic compound eyes. Then the



obtained transgenic silkworm lines harboring the anti-CD20 mAb H chain or L chain gene under regulation of a UAS sequence were mated with adults from the Ser1-GAL4 strain,<sup>38</sup> which carried a GAL4 gene driven by the sericin1 promoter and a 3 × P3-DsRed2 marker cassette. The F1 embryos that harbored both the GAL4 construct and the UAS construct were selected based on fluorescence of DsRed2 and EYFP or AmCyan. These F1 adults were mated with each other, and embryos that expressed DsRed2, EYFP, and AmCyan in their eyes were selected to obtain transgenic silkworms that expressed both the anti-CD20 mAb H chain and L chain.

#### Extraction of proteins from MSGs and cocoons

MSGs were isolated from larvae on the sixth day of the fifth instar, then immersed in 1 ml extraction buffer (phosphate-buffered saline, pH 7.2, containing 1% Triton X-100), and gently shaken for 2 h at 4°C. Each resulting extract was frozen at -80°C for one day and thawed at 4°C; debris was then removed from each extract by filtration. Cocoons were cut into small pieces of approximately 1 cm<sup>2</sup> and suspended in the same buffer that was used for MSGs and gently shaken for 12 h at 4°C; for each 50 mg of cocoon pieces, 1 ml of buffer was used. Each resulting cocoon extract was frozen at -80°C for one day and thawed at 4°C; debris was then removed from each extract by filtration.

#### SDS-PAGE and western blotting analysis

SDS-PAGE and western blotting analysis were carried out as described previously.<sup>38</sup> Protein lysates extracted from MSGs or cocoons were prepared and separated in 4–12% gradient gels (NuPAGE BisTris gel; Life Technologies) according to manufacturer's instructions. An anti-Human IgG (H+L) antibody (ROCKLAND) and horseradish peroxidase-conjugated anti-rabbit IgG antibody (GE Healthcare) were used as the primary and second antibodies, respectively. Each band of immuno-reactive proteins was detected with ECL prime (GE Healthcare) and an LAS-3000 image analyzer (Fuji Film).

#### Antibody purification

MSGs or cocoons were collected from transgenic silkworms stably expressing anti-CD20 mAbs, and suspended in phosphate-buffered saline (PBS) containing 1% Triton-X. Soluble protein lysates were collected by centrifugation and applied to a HiTrap Protein G HP column (GE Healthcare) equilibrated with 20 mM phosphate buffer (pH 6.8). After the column was washed with 20 mM phosphate buffer (pH 6.8), mAbs were eluted by 0.1M Glycine-HCl (pH 3.0) and neutralized by 1 M Tris-HCl (pH 8.0), followed by desalting using a PD-10 column

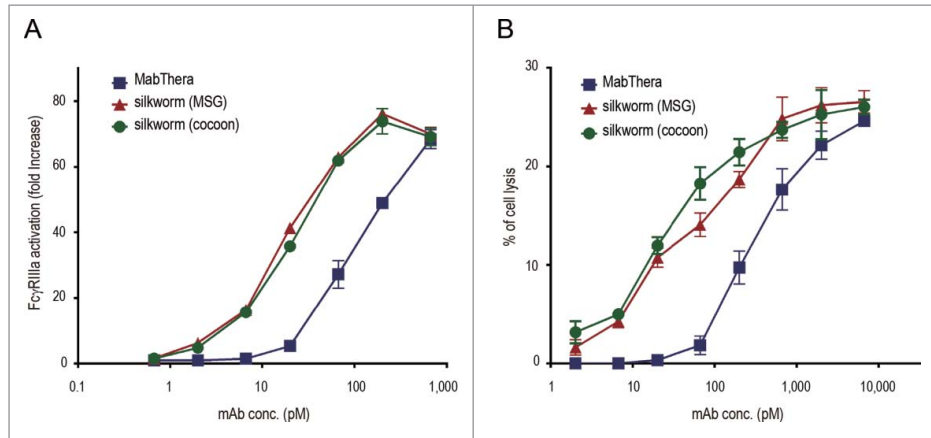


**Figure 6.** FcγRIIIa activation and antibody-dependent cell-mediated cytotoxicity (ADCC). (A) CD20 binding-dependent activation of FcγRIIIa was measured by using Daudi (target) and Jurkat/FcγRIIIa/NFAT-Luc (effector) cells. Fold increases in luciferase activity were plotted against the mAbs concentration (n = 3, bars indicate SEM). (B) The levels of ADCC against Daudi cells were measured by using human PBMCs as effector cells. The percentages of cell lysis were plotted against the mAbs concentration (n = 3, bars indicate SEM).

(GE Healthcare) equilibrated with PBS. To remove residual Triton-X, the collected samples were processed with Pierce Detergent Removal Resin (Thermo Scientific). The concentration of purified mAb was determined by spectrophotometry using a NanoDrop 2000c spectrophotometer (Thermo Scientific).

#### CD20-binding assay

Daudi (JCRB9071) cells were obtained from the JCRB Cell Bank and cultured in RPMI1640 medium supplemented with 20% FBS. After washing twice with the binding buffer (PBS containing 0.5% bovine serum albumin, 2 mM Na-EDTA and

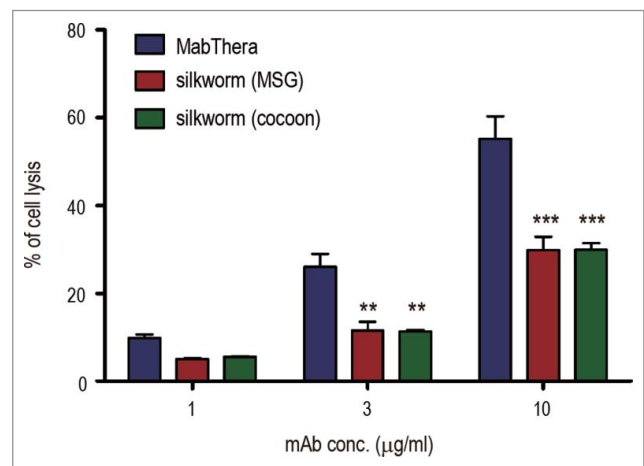


**Figure 7.** Complement-dependent cytotoxicity (CDC). Daudi cells were cultured in the presence of human serum (16%) and anti-CD20 mAbs (1, 3 or 10 μg/ml). The percentages of 7-AAD positive-dead cells were calculated by flow cytometric analysis and represented as the mean + SEM (n = 3). \*\*, p < 0.01; \*\*\*, p < 0.001.

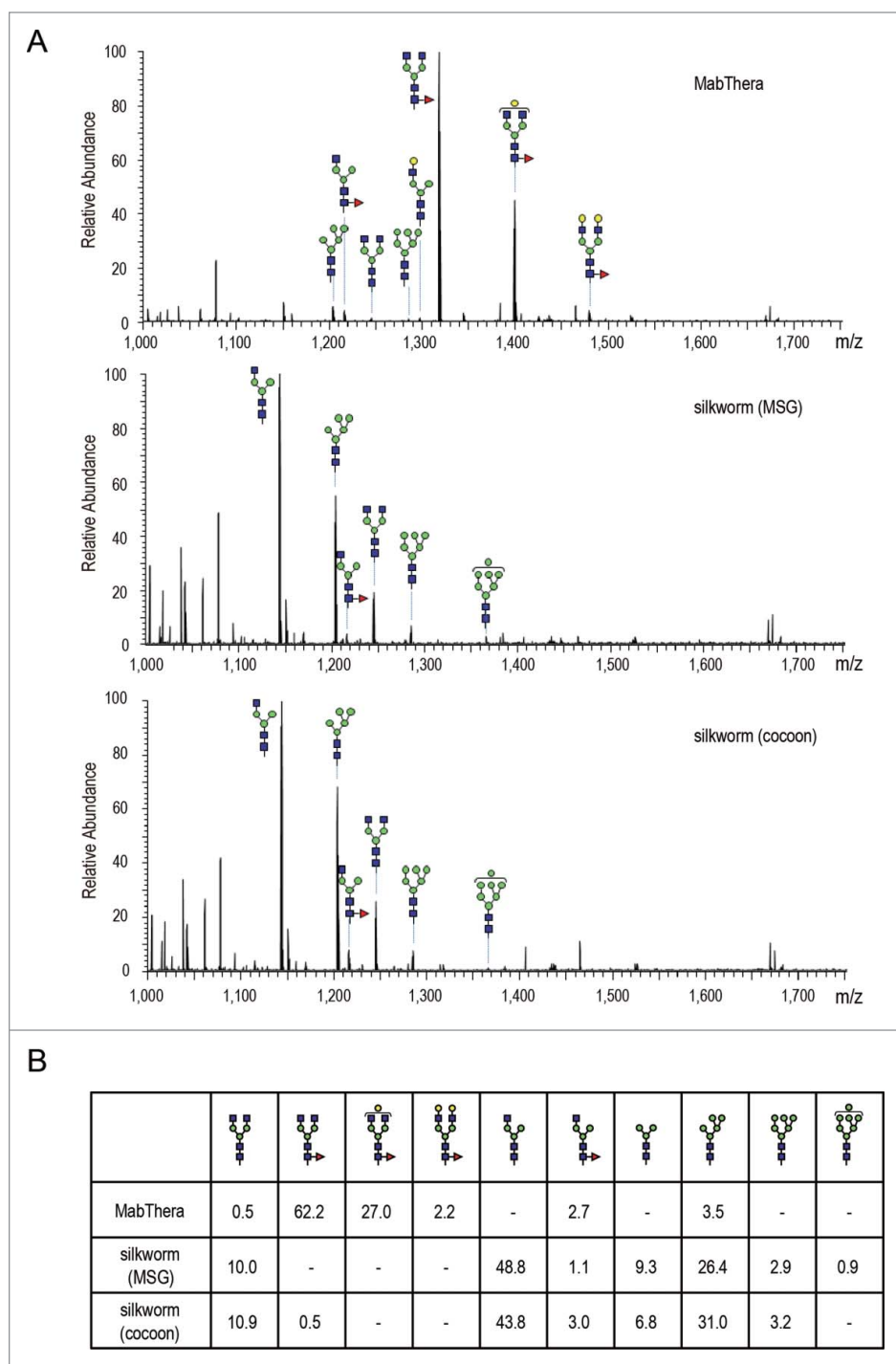


**Figure 8.** Fc glycosylation analysis of anti-CD20 mAbs. **(A)** Comparison of mass spectra acquired at the elution point of the glycopeptides of EEQYNSTYR, corresponding to 293–301 amino acids (EU numbering) in the heavy chain of anti-CD20 mAbs. **(B)** Percentage distributions of glycoforms were calculated by the relative peak area average values. Symbols: blue square, N-acetylglucosamine; green circle, mannose; yellow circle, galactose; red triangle, fucose.

0.05% sodium azide), the cells were resuspended in the binding buffer containing serially diluted anti-CD20 mAbs and incubated on ice for 30 min. The cells were washed twice with the binding buffer, and incubated with the binding buffer containing

Alexa488-conjugated  $F(ab')_2$  anti-human IgG Fc (Jackson ImmunoResearch) on ice for 30 min. After washing twice with the binding buffer, the cells were analyzed by using a FACSCanto II flow cytometer (BD Biosciences).

For competitive binding assay, MabThera was labeled with DyLight 488 by using DyLight 488 Antibody Labeling Kit (PIERCE) according to the manufacturer's instruction. The labeling efficiency was calculated based on the absorbance at 280 and 493 nm. The average number of DyLight 488 per MabThera was 3.3. After washing with the binding buffer, Daudi cells were resuspended in the binding buffer containing DyLight 488-labeled MabThera and serially diluted unlabeled mAbs. Cetuximab, which targets the epidermal growth factor receptor, was used as control IgG. After incubating for 30 min on ice, the cells were washed twice with the binding buffer and analyzed by using a FACSCanto II flow cytometer. Percentages of DyLight 488-labeled MabThera binding were calculated by the mean fluorescence intensities.

### SPR analysis

A Biacore T200 SPR biosensor (GE Healthcare) and CM5 sensor chip were used to evaluate the binding properties of mAbs. For measurement of the binding affinity with FcγRs, recombinant ectodomains of human FcγRs with a C-terminal polyhistidine tags (Sino Biological) were captured on an anti-polyhistidine antibody-immobilized sensorchip. Serially diluted anti-CD20 mAbs were injected into the flow cells and association and dissociation were monitored. The dissociation constant  $K_D$  was calculated using the 1:1 binding model. The binding affinity of mAbs with FcRn was measured as described previously.<sup>42</sup> Because FcRn binds independently to both sites of the IgG homodimer,<sup>74</sup> the dissociation constant  $K_D$  was analyzed by using bivalent model. In all experiments, each binding sensorgram from the sample flow cell was corrected for both the surface blank and the buffer injection control (double reference).<sup>75</sup>

Statistical analysis was performed using one-way analysis of variance (ANOVA) with Tukey's multiple comparison test (PRISM version 5.02; Graphpad Software). All experiments were performed independently at least 3 times and representative data are shown.

### FcγR reporter assay

The activation of FcγRIIIa by anti-CD20 mAbs was measured by using Jurkat/FcγRIIIa/NFAT-Luc reporter cells as described previously.<sup>44</sup> Briefly, Daudi and Jurkat/FcγRIIIa/NFAT-Luc cells suspended in Opti-MEM I Reduced Serum Media (Invitrogen) (effector/target ratio, 10:1) were seeded in a 96-well plate with serially diluted anti-CD20 mAbs. After incubation for 5 h at 37°C, we measured the luciferase activities by using a ONE-Glo Luciferase Assay System (Promega) and an EnSpire Multimode Plate Reader (PerkinElmer).

### ADCC assay

Cryopreserved human PBMCs (Cellular Technology Limited) were thawed just before the assay according to the manufacturer's protocol. Daudi and human PBMCs suspended in CTL-Test Medium (effector/target ratio, 20:1) were co-cultured in the presence of serially diluted anti-CD20 mAbs. After incubation for 4 h at 37°C, the lactate dehydrogenase (LDH) activity of the cell culture supernatants was measured by using a Cytotoxicity Detection Kit<sup>PLUS</sup> (LDH) (Roche Applied Science). The percentage cytotoxicity was calculated as described in the manufacturer's protocol.

### CDC assay

Daudi cells were cultured in Opti-MEM I Reduced Serum Media containing 16% human AB serum (SIGMA) and serially diluted anti-CD20 mAbs. After incubation for 2 h at 37°C, the cells were stained with 7-AAD (BD Biosciences). The percentages of 7-AAD positive-dead cells were analyzed by using a FACSCanto II flow cytometer.

### Peptide mapping by LC/MS/MS

Peptide mapping of anti-CD20 mAbs was performed by using LC/MS/MS as described previously.<sup>76</sup> Briefly, anti-CD20 mAbs were reduced by dithiothreitol and carboxymethylated by sodium monoiodoacetate, followed by digestion with modified trypsin (Promega). Tryptic digests (~0.5 μg) were analyzed by LC/MS/MS. HPLC was performed on an UltiMate 3000 RSLCnano LC System (Dionex) equipped with an L-

Column2 ODS (0.075 mm × 150 mm, 3 μm; CERI) at a flow rate of 0.3 μl/min. The eluents consisted of water containing 2% (v/v) acetonitrile and 0.1% (v/v) formic acid (pump A) and 90% acetonitrile containing 0.1% formic acid (pump B). The samples were eluted with 5% of pump B for 3 min followed by a linear gradient of from 5% to 60% of pump B over 60 min. Mass spectrometric analyses were performed using an LTQ-FT mass spectrometer (Thermo Fisher Scientific) equipped with an XYZ nano-electrospray ionization stage (AMR). The mass spectrometer was operated in positive ion mode and full mass spectra were acquired using an *m/z* range of 400–2000. Following every regular mass acquisition, we performed MS/MS acquisitions against the 3 most intense ions by using a data-dependent acquisition method with collision energy of 35%. The percentage distribution of the glycopeptides was calculated using the peak area average values.

### Disclosure of Potential Conflicts of Interest

No potential conflicts of interest were disclosed.

### Acknowledgments

We thank Dr. Hisanori Bando (Hokkaido University) for providing pGEM-hr5, and Ms. Chizuru Miyama for technical assistance.

### Funding

This study was supported in part by the "Research on Regulatory Harmonization and Evaluation of Pharmaceuticals, Medical Devices, Regenerative and Cellular Therapy Products, Gene Therapy Products, and Cosmetics" and "Research on Development of New Drugs" from Japan Agency for Medical Research and development (AMED), by the Health and Labor Sciences Research Grants from the Ministry of Health, Labor, and Welfare of Japan, and by the Advanced Research for Medical Products Mining Programme of the National Institute of Biomedical Innovation (NIBIO).

### Supplemental Material

Supplemental data for this article can be accessed on the publisher's website

### References

1. Chan AC, Carter PJ. Therapeutic antibodies for autoimmunity and inflammation. *Nat Rev Immunol* 2010; 10:301-16; PMID:20414204; <http://dx.doi.org/10.1038/nri2761>
2. Nelson AL, Dhimolea E, Reichert JM. Development trends for human monoclonal antibody therapeutics. *Nat Rev Drug Discov* 2010; 9:767-74; PMID:20811384; <http://dx.doi.org/10.1038/nrd3229>
3. Reichert JM. Marketed therapeutic antibodies compendium. *MAbs* 2012; 4:413-5; PMID:22531442; <http://dx.doi.org/10.4161/mabs.19931>
4. Scott AM, Wolchok JD, Old LJ. Antibody therapy of cancer. *Nat Rev Cancer* 2012; 12:278-87; PMID:22437872; <http://dx.doi.org/10.1038/nrc3236>
5. Ghaderi D, Zhang M, Hurtado-Ziola N, Varki A. Production platforms for biotherapeutic glycoproteins. Occurrence, impact, and challenges of non-human sialylation. *Biotechnol Genet Eng Rev* 2012; 28:147-75; PMID:22616486; <http://dx.doi.org/10.5661/bger-28-147>
6. Zhang RY, Shen WD. Monoclonal antibody expression in mammalian cells. *Methods Mol Biol* 2012; 907:341-58; PMID:22907362; [http://dx.doi.org/10.1007/978-1-61779-974-7\\_20](http://dx.doi.org/10.1007/978-1-61779-974-7_20)
7. Kim JY, Kim YG, Lee GM. CHO cells in biotechnology for production of recombinant proteins: current state and further potential. *Appl Microbiol Biotechnol* 2012; 93:917-30; PMID:22159888; <http://dx.doi.org/10.1007/s00253-011-3758-5>
8. Houdebine LM. Production of pharmaceutical proteins by transgenic animals. *Comp Immunol Microbiol Infect Dis* 2009; 32:107-21; PMID:18243312; <http://dx.doi.org/10.1016/j.cimid.2007.11.005>
9. Maksimenko OG, Deykin AV, Khodorovich YM, Georgiev PG. Use of transgenic animals in biotechnology: prospects and problems. *Acta Naturae* 2013; 5:33-46; PMID:23556129



10. Wang Y, Zhao S, Bai L, Fan J, Liu E. Expression systems and species used for transgenic animal bioreactors. *Biomed Res Int* 2013; 2013:580463; PMID:23586046
11. De Muyck B, Navarre C, Boutry M. Production of antibodies in plants: status after twenty years. *Plant Biotechnol J* 2010; 8:529-63; PMID:20132515; <http://dx.doi.org/10.1111/j.1467-7652.2009.00494.x>
12. Karg SR, Kallio PT. The production of biopharmaceuticals in plant systems. *Biotechnol Adv* 2009; 27:879-94; PMID:19647060; <http://dx.doi.org/10.1016/j.biotechadv.2009.07.002>
13. Adiguzel C, Iqbal O, Demir M, Fareed J. European community and US-FDA approval of recombinant human antithrombin produced in genetically altered goats. *Clin Appl Thromb Hemost* 2009; 15:645-51; PMID:19850586; <http://dx.doi.org/10.1177/1076029609339748>
14. Kling J. First US approval for a transgenic animal drug. *Nat Biotechnol* 2009; 27:302-4; PMID:19352350; <http://dx.doi.org/10.1038/nbt0409-302>
15. Haddley K. Taliglucerase alfa for the treatment of Gaucher's disease. *Drugs Today (Barc)* 2012; 48:525-32; PMID:22916340; <http://dx.doi.org/10.1358/dot.2012.48.4.1788435>
16. Grabowski GA, Golembo M, Shaaltiel Y. Taliglucerase alfa: an enzyme replacement therapy using plant cell expression technology. *Mol Genet Metab* 2014; 112:1-8; PMID:24630271; <http://dx.doi.org/10.1016/j.ymgme.2014.02.011>
17. Pollock DP, Kutzko JP, Birc-Kelley E, Williams JL, Echelard Y, Meade HM. Transgenic milk as a method for the production of recombinant antibodies. *J Immunol Methods* 1999; 231:147-57; PMID:10648934; [http://dx.doi.org/10.1016/S0022-1759\(99\)00151-9](http://dx.doi.org/10.1016/S0022-1759(99)00151-9)
18. Zhu L, van de Lavoie MC, Albanese J, Beenhouwer DO, Cardarelli PM, Cuisson S, Deng DF, Deshpande S, Diamond JH, Green L, et al. Production of human monoclonal antibody in eggs of chimeric chickens. *Nat Biotechnol* 2005; 23:1159-69; PMID:16127450; <http://dx.doi.org/10.1038/nbt1132>
19. Garabagi F, McLean MD, Hall JC. Transient and stable expression of antibodies in Nicotiana species. *Methods Mol Biol* 2012; 907:389-408; PMID:22907365; [http://dx.doi.org/10.1007/978-1-61779-974-7\\_23](http://dx.doi.org/10.1007/978-1-61779-974-7_23)
20. Rodriguez M, Perez L, Gavilondo JV, Garrido G, Bequet-Romero M, Hernandez I, Huerta V, Cabrera G, Pérez M, Ramos O, et al. Comparative in vitro and experimental in vivo studies of the anti-epidermal growth factor receptor antibody nimotuzumab and its aglycosylated form produced in transgenic tobacco plants. *Plant Biotechnol J* 2013; 11:53-65; PMID:23046448; <http://dx.doi.org/10.1111/pbi.12006>
21. Schuster M, Jost W, Mudde GC, Wiederkum S, Schwager C, Janzek E, Altmann F, Stadlmann J, Stemmer C, Gorr G. In vivo glyco-engineered antibody with improved lytic potential produced by an innovative non-mammalian expression system. *Biotechnol J* 2007; 2:700-8; PMID:17427997; <http://dx.doi.org/10.1002/biot.200600255>
22. Kircheis R, Halanek N, Koller I, Jost W, Schuster M, Gorr G, Hajszan K, Nechansky A. Correlation of ADCC activity with cytokine release induced by the stably expressed, glyco-engineered humanized Lewis Y-specific monoclonal antibody MB314. *MAbs* 2012; 4:532-41; PMID:22665069; <http://dx.doi.org/10.4161/mabs.20577>
23. Decker EL, Parsons J, Reski R. Glyco-engineering for biopharmaceutical production in moss bioreactors. *Front Plant Sci* 2014; 5:346; PMID:25071817; <http://dx.doi.org/10.3389/fpls.2014.00346>
24. Cox KM, Sterling JD, Regan JT, Gasdaska JR, Frantz KK, Peele CG, Black A, Passmore D, Moldovan-Loomis C, Srinivasan M, et al. Glycan optimization of a human monoclonal antibody in the aquatic plant *Lemma minor*. *Nat Biotechnol* 2006; 24:1591-7; PMID:17128273; <http://dx.doi.org/10.1038/nbt1260>
25. Banno Y, Shimada T, Kajiyura Z, Sezutsu H. The silkworm-an attractive BioResource supplied by Japan. *Exp Anim* 2010; 59:139-46; PMID:20484847; <http://dx.doi.org/10.1538/expanim.59.139>
26. Kato T, Kajikawa M, Maenaka K, Park EY. Silkworm expression system as a platform technology in life science. *Appl Microbiol Biotechnol* 2010; 85:459-70; PMID:19830419; <http://dx.doi.org/10.1007/s00253-009-2267-2>
27. Usami A, Suzuki T, Nagaya H, Kaki H, Ishiyama S. Silkworm as a host of baculovirus expression. *Curr Pharm Biotechnol* 2010; 11:246-50; PMID:20210748; <http://dx.doi.org/10.2174/138920110791112013>
28. Tomita M. Transgenic silkworms that weave recombinant proteins into silk cocoons. *Biotechnol Lett* 2011; 33:645-54; PMID:21184136; <http://dx.doi.org/10.1007/s10529-010-0498-z>
29. Usami A, Ishiyama S, Enomoto C, Okazaki H, Higuchi K, Ikeda M, Yamamoto T, Sugai M, Ishikawa Y, Hosaka Y, et al. Comparison of recombinant protein expression in a baculovirus system in insect cells (SF9) and silkworm. *J Biochem* 2011; 149:219-27; PMID:21113054; <http://dx.doi.org/10.1093/jb/mvq138>
30. Ueda Y, Sakurai T, Yanai A. Homogeneous production of feline interferon in silkworm by replacing single amino acid code in signal peptide region in recombinant baculovirus and characterization of the product. *J Vet Med Sci* 1993; 55:251-8; PMID:7685640; <http://dx.doi.org/10.1292/jvms.55.251>
31. Okano F, Satoh M, Ido T, Okamoto N, Yamada K. Production of canine IFN-gamma in silkworm by recombinant baculovirus and characterization of the product. *J Interferon Cytokine Res* 2000; 20:1015-22; PMID:11096459; <http://dx.doi.org/10.1089/10799900050198462>
32. Tamura T, Thibert C, Royer C, Kanda T, Abraham E, Kamba M, Komoto N, Thomas JL, Mauchamp B, Chavancy G, et al. Germline transformation of the silkworm *Bombyx mori* L. using a piggyBac transposon-derived vector. *Nat Biotechnol* 2000; 18:81-4; PMID:10625397; <http://dx.doi.org/10.1038/71978>
33. Wurm FM. Human therapeutic proteins from silkworms. *Nat Biotechnol* 2003; 21:34-5; PMID:12511906; <http://dx.doi.org/10.1038/nbt0103-34>
34. Tomita M, Munetsuna H, Sato T, Adachi T, Hino R, Hayashi M, Shimizu K, Nakamura N, Tamura T, Yoshizato K. Transgenic silkworms produce recombinant human type III procollagen in cocoons. *Nat Biotechnol* 2003; 21:52-6; PMID:12483223; <http://dx.doi.org/10.1038/nbt771>
35. Hino R, Tomita M, Yoshizato K. The generation of germline transgenic silkworms for the production of biologically active recombinant fusion proteins of fibroin and human basic fibroblast growth factor. *Biomaterials* 2006; 27:5715-24; PMID:16905183; <http://dx.doi.org/10.1016/j.biomaterials.2006.07.028>
36. Ogawa S, Tomita M, Shimizu K, Yoshizato K. Generation of a transgenic silkworm that secretes recombinant proteins in the sericin layer of cocoon: production of recombinant human serum albumin. *J Biotechnol* 2007; 128:531-44; PMID:17166611; <http://dx.doi.org/10.1016/j.jbiotec.2006.10.019>
37. Iizuka M, Ogawa S, Takeuchi A, Nakakita S, Kubo Y, Miyawaki Y, Hirabayashi J, Tomita M. Production of a recombinant mouse monoclonal antibody in transgenic silkworm cocoons. *FEBS J* 2009; 276:5806-20; PMID:19740109; <http://dx.doi.org/10.1111/j.1742-4658.2009.07262.x>
38. Tatematsu K, Kobayashi I, Uchino K, Sezutsu H, Iizuka T, Yonemura N, Tamura T. Construction of a binary transgenic gene expression system for recombinant protein production in the middle silk gland of the silkworm *Bombyx mori*. *Transgenic Res* 2010; 19:473-87; PMID:19789990; <http://dx.doi.org/10.1007/s11248-009-9328-2>
39. Nimmerjahn F, Ravetch JV. Fc gamma receptors as regulators of immune responses. *Nat Rev Immunol* 2008; 8:34-47; PMID:18064051; <http://dx.doi.org/10.1038/nri2206>
40. Kuo TT, Aveson VG. Neonatal Fc receptor and IgG-based therapeutics. *MAbs* 2011; 3:422-30; PMID:22048693; <http://dx.doi.org/10.4161/mabs.3.5.16983>
41. Rath T, Kuo TT, Baker K, Qiao SW, Kobayashi K, Yoshida M, Roopenian D, Fiebiger E, Lencer WI, Blumberg RS. The immunologic functions of the neonatal Fc receptor for IgG. *J Clin Immunol* 2013; 33 Suppl 1:S9-17; PMID:22948741; <http://dx.doi.org/10.1007/s10875-012-9768-y>
42. Suzuki T, Ishii-Watabe A, Tada M, Kobayashi T, Kanayasu-Toyoda T, Kawanishi T, Yamaguchi T. Importance of neonatal FcR in regulating the serum half-life of therapeutic proteins containing the Fc domain of human IgG1: a comparative study of the affinity of monoclonal antibodies and Fc-fusion proteins to human neonatal FcR. *J Immunol* 2010; 184:1968-76; PMID:20083659; <http://dx.doi.org/10.4049/jimmunol.0903296>
43. Maloney DG. Anti-CD20 antibody therapy for B-cell lymphomas. *N Engl J Med* 2012; 366:2008-16; PMID:22621628; <http://dx.doi.org/10.1056/NEJMc1114348>
44. Tada M, Ishii-Watabe A, Suzuki T, Kawasaki N. Development of a cell-based assay measuring the activation of Fc gammaRIIIa for the characterization of therapeutic monoclonal antibodies. *PLoS One* 2014; 9:e95787; PMID:24752341; <http://dx.doi.org/10.1371/journal.pone.0095787>
45. Kawasaki N, Itoh S, Hashii N, Takakura D, Qin Y, Huang X, Yamaguchi T. The significance of glycosylation analysis in development of biopharmaceuticals. *Biol Pharm Bull* 2009; 32:796-800; PMID:19420744; <http://dx.doi.org/10.1248/bpb.32.796>
46. Sola RJ, Griebenow K. Glycosylation of therapeutic proteins: an effective strategy to optimize efficacy. *BioDrugs* 2010; 24:9-21; PMID:20055529; <http://dx.doi.org/10.2165/11530550-000000000-00000>
47. Costa AR, Rodrigues ME, Henriques M, Oliveira R, Azeredo J. Glycosylation: impact, control and improvement during therapeutic protein production. *Crit Rev Biotechnol* 2014; 34:281-99; PMID:23919242; <http://dx.doi.org/10.3109/07388551.2013.793649>
48. Mizuoichi T, Taniguchi T, Shimizu A, Kobata A. Structural and numerical variations of the carbohydrate moiety of immunoglobulin G. *J Immunol* 1982; 129:2016-20; PMID:6811655
49. Jefferis R. Glycosylation as a strategy to improve antibody-based therapeutics. *Nat Rev Drug Discov* 2009; 8:226-34; PMID:19247305; <http://dx.doi.org/10.1038/nrd2804>
50. Hristodorov D, Fischer R, Linden L. With or without sugar? (Aglycosylation of therapeutic antibodies. *Mol Biotechnol* 2013; 54:1056-68; PMID:23097175; <http://dx.doi.org/10.1007/s12033-012-9612-x>
51. Shields RL, Lai J, Keck R, O'Connell LY, Hong K, Meng YG, Weikert SH, Presta LG. Lack of fucose on human IgG1 N-linked oligosaccharide improves binding to human Fc gamma RIII and antibody-dependent cellular toxicity. *J Biol Chem* 2002; 277:26733-40; PMID:11986321; <http://dx.doi.org/10.1074/jbc.M202069200>
52. Shinkawa T, Nakamura K, Yamane N, Shoji-Hosaka E, Kanda Y, Sakurada M, Uchida K, Anazawa H, Satoh M, Yamasaki M, et al. The absence of fucose but not the presence of galactose or bisecting N-acetylglucosamine of human IgG1 complex-type oligosaccharides shows the critical role of enhancing antibody-dependent cellular cytotoxicity. *J Biol Chem* 2003; 278:3466-73; PMID:12427744; <http://dx.doi.org/10.1074/jbc.M210665200>
53. Boyd PN, Lines AC, Patel AK. The effect of the removal of sialic acid, galactose and total carbohydrate on the functional activity of Campath-1H. *Mol Immunol* 1995; 32:1311-8; PMID:8643100; [http://dx.doi.org/10.1016/0161-5890\(95\)00118-2](http://dx.doi.org/10.1016/0161-5890(95)00118-2)
54. Hodonickzy J, Zheng YZ, James DC. Control of recombinant monoclonal antibody effector functions



- by Fc N-glycan remodeling in vitro. *Biotechnol Prog* 2005; 21:1644-52; PMID:16321047; <http://dx.doi.org/10.1021/bp050228w>
55. Raju TS. Terminal sugars of Fc glycans influence antibody effector functions of IgGs. *Curr Opin Immunol* 2008; 20:471-8; PMID:18606225; <http://dx.doi.org/10.1016/j.coi.2008.06.007>
  56. Park EY, Ishikiriyama M, Nishina T, Kato T, Yagi H, Kato K, Yagi H, Kato K, Ueda H. Human IgG1 expression in silkworm larval hemolymph using BmNPV bacmids and its N-linked glycan structure. *J Biotechnol* 2009; 139:108-14; PMID:18984019; <http://dx.doi.org/10.1016/j.jbiotec.2008.09.013>
  57. Dojima T, Nishina T, Kato T, Uno T, Yagi H, Kato K, Ueda H, Park EY. Improved secretion of molecular chaperone-assisted human IgG in silkworm, and no alterations in their N-linked glycan structures. *Biotechnol Prog* 2010; 26:232-8; PMID:19918885
  58. Tawara T, Hasegawa K, Sugiura Y, Harada K, Miura T, Hayashi S, Tahara T, Ishikawa M, Yoshida H, Kubo K, et al. Complement activation plays a key role in antibody-induced infusion toxicity in monkeys and rats. *J Immunol* 2008; 180:2294-8; PMID:18250438; <http://dx.doi.org/10.4049/jimmunol.180.4.2294>
  59. van der Kolk LE, Grillo-Lopez AJ, Baars JW, Hack CE, van Oers MH. Complement activation plays a key role in the side-effects of rituximab treatment. *Br J Haematol* 2001; 115:807-11; PMID:11843813; <http://dx.doi.org/10.1046/j.1365-2141.2001.03166.x>
  60. Fukuda MN, Sasaki H, Lopez L, Fukuda M. Survival of recombinant erythropoietin in the circulation: the role of carbohydrates. *Blood* 1989; 73:84-9; PMID:2910371
  61. Imai N, Higuchi M, Kawamura A, Tomonoh K, Oh-Eda M, Fujiwara M, Shimonaka Y, Ochi N. Physicochemical and biological characterization of asialoerythropoietin. Suppressing effects of sialic acid in the expression of biological activity of human erythropoietin in vitro. *Eur J Biochem* 1990; 194:457-62; PMID:2269277; <http://dx.doi.org/10.1111/j.1432-1033.1990.tb15639.x>
  62. Elliott S, Lorenzini T, Asher S, Aoki K, Brankow D, Buck L, Busse L, Chang D, Fuller J, Grant J, et al. Enhancement of therapeutic protein in vivo activities through glycoengineering. *Nat Biotechnol* 2003; 21:414-21; PMID:12612588; <http://dx.doi.org/10.1038/nbt799>
  63. Lee K, Jin X, Zhang K, Copertino L, Andrews L, Baker-Malcolm J, Geagan L, Qiu H, Seiger K, Barngröver D, et al. A biochemical and pharmacological comparison of enzyme replacement therapies for the glycolipid storage disorder Fabry disease. *Glycobiology* 2003; 13:305-13; PMID:12626384; <http://dx.doi.org/10.1093/glycob/cwg034>
  64. Desnick RJ, Schuchman EH. Enzyme replacement therapy for lysosomal diseases: lessons from 20 years of experience and remaining challenges. *Annu Rev Genomics Hum Genet* 2012; 13:307-35; PMID:22970722; <http://dx.doi.org/10.1146/annurev-genom-090711-163739>
  65. Altmann F, Staudacher E, Wilson IB, Marz L. Insect cells as hosts for the expression of recombinant glycoproteins. *Glycoconj J* 1999; 16:109-23; PMID:10612411; <http://dx.doi.org/10.1023/A:1026488408951>
  66. Shi X, Jarvis DL. Protein N-glycosylation in the baculovirus-insect cell system. *Curr Drug Targets* 2007; 8:1116-25; PMID:17979671; <http://dx.doi.org/10.2174/138945007782151360>
  67. Simmons LC, Reilly D, Klimowski L, Raju TS, Meng G, Sims P, Hong K, Shields RL, Damico LA, Rancatore P, et al. Expression of full-length immunoglobulins in *Escherichia coli*: rapid and efficient production of aglycosylated antibodies. *J Immunol Methods* 2002; 263:133-47; PMID:12009210; [http://dx.doi.org/10.1016/S0022-1759\(02\)00036-4](http://dx.doi.org/10.1016/S0022-1759(02)00036-4)
  68. Kanda Y, Yamada T, Mori K, Okazaki A, Inoue M, Kitajima-Miyama K, Kuni-Kamochi R, Nakano R, Yano K, Kakita S, et al. Comparison of biological activity among nonfucosylated therapeutic IgG1 antibodies with three different N-linked Fc oligosaccharides: the high-mannose, hybrid, and complex types. *Glycobiology* 2007; 17:104-18; PMID:17012310; <http://dx.doi.org/10.1093/glycob/cwl057>
  69. Goetze AM, Liu YD, Zhang Z, Shah B, Lee E, Bondarenko PV, Flynn GC. High-mannose glycans on the Fc region of therapeutic IgG antibodies increase serum clearance in humans. *Glycobiology* 2011; 21:949-59; PMID:21421994; <http://dx.doi.org/10.1093/glycob/cwr027>
  70. Alessandri L, Ouellette D, Acquah A, Rieser M, Leblond D, Saltarelli M, Radziejewski C, Fujimori T, Correia I. Increased serum clearance of oligomannose species present on a human IgG1 molecule. *MAbs* 2012; 4:509-20; PMID:22669558; <http://dx.doi.org/10.4161/mabs.20450>
  71. van Beers MM, Bardor M. Minimizing immunogenicity of biopharmaceuticals by controlling critical quality attributes of proteins. *Biotechnol J* 2012; 7:1473-84; PMID:23027660; <http://dx.doi.org/10.1002/biot.201200065>
  72. Uchino K, Imamura M, Sezutsu H, Kobayashi I, Kojima K, Kanda T, Tshiki T. Evaluating promoter sequences for trapping an enhancer activity in the silkworm *bombyx mori*. *J Insect Biotechnol Sericol* 2006; 75:89-97
  73. Tatematsu K-I, Uchino K, Sezutsu H, Tamura T. Effect of ATG initiation codon context motifs on the efficiency of translation of mRNA derived from exogenous genes in the transgenic silkworm, *Bombyx mori*. *SpringerPlus* 2014; 3:136; PMID:25674439; <http://dx.doi.org/10.1186/2193-1801-3-136>
  74. Abdiche YN, Yeung YA, Chaparro-Riggers J, Barman I, Strop P, Chin SM, Pham A, Bolton G, McDonough D, Lindquist K, et al. The neonatal Fc receptor (FcRn) binds independently to both sites of the IgG homodimer with identical affinity. *MAbs* 2015; 7:331-43; PMID:25658443
  75. Myszkowski DG. Improving biosensor analysis. *J Mol Recognit* 1999; 12:279-84; PMID:10556875; [http://dx.doi.org/10.1002/\(SICI\)1099-1352\(199909/10\)12:5%3c279::AID-JMR473%3e3.0.CO;2-3](http://dx.doi.org/10.1002/(SICI)1099-1352(199909/10)12:5%3c279::AID-JMR473%3e3.0.CO;2-3)
  76. Harazono A, Kawasaki N, Itoh S, Hashii N, Matsuishi-Nakajima Y, Kawanishi T, Yamaguchi T. Simultaneous glycosylation analysis of human serum glycoproteins by high-performance liquid chromatography/tandem mass spectrometry. *J Chromatogr B Analyt Technol Biomed Life Sci* 2008; 869:20-30; PMID:18514042; <http://dx.doi.org/10.1016/j.jchromb.2008.05.006>